

Evaluation Method of Magnetic Sensors Using the Calibrated Phantom for Magnetoencephalography

D. Oyama, Y. Adachi, and G. Uehara

Applied Electronics Laboratory, Kanazawa Institute of Technology, *Amaike 3, Kanazawa, Ishikawa 920-1331, Japan*

In recent years, many kinds of magnetic sensors have been developed for biomagnetic measurement, such as magnetocardiography (MCG) and magnetoencephalography (MEG). However, it is difficult to evaluate their performance using only actual MCG or MEG measurements. In this paper, we propose the use of the calibrated MEG phantom for quantitative evaluation of magnetic sensors and present the experimental method. We choose a magneto-impedance (MI) sensor as an example of the magnetic sensor to be evaluated. The magnetic field distribution near the phantom was measured using the MI sensor and a signal source was localized with different averaging numbers and different signal source intensities. The results suggest that the MEG signal cannot be observed in the usual averaging time (i.e., 100), even when the sensor is located near the head; 4.0 mm of source localization accuracy can be achieved with 400-times averaging if the sensor noise decreases to 1/10. The use of the calibrated phantom, instead of examination with human subjects, is effective for quantitative evaluation of the performance of magnetic sensors.

Key words: magnetoencephalography, phantom, magneto-impedance sensor

1. Introduction

Biomagnetic signal measurements, such as magnetoencephalography (MEG) and magnetocardiography (MCG) are utilized in clinical applications and neuroscience studies. The magnetic signals from the brain and heart are very weak; therefore, superconducting quantum interference device (SQUID) sensors have been used for practical MEG and MCG systems for which the sensitivity is less than $10 \text{ fT/Hz}^{1/2}$. On the other hand, SQUID sensors must be cooled by liquid helium to maintain superconductivity. Helium-less MCG or MEG systems are important because of the cost and low availability of liquid helium.

In recent years, the development of refrigerant-less or room-temperature magnetic sensors has advanced, with the aim of realizing new biomagnetic measurement systems. Some groups have succeeded in detecting the magnetic signal from the human heart or brain¹⁻⁶⁾, and practical applications are expected.

However, the evaluation of such magnetic sensors is difficult with actual MCG or MEG measurement, because there is no guarantee of reproducibility or reliability of the signal sources. Objective evidence is important to prove the effectiveness of newly developed sensors. Additionally, quantitative evaluation is necessary for designing the biomagnetic measurement system using these sensors.

Therefore, the authors propose the use of a phantom for the evaluation of the newly developed magnetic sensors. A phantom is an artificial object that imitates the human body. Quantitative evaluation can be achieved using phantom experiments instead of examination of a human subject. The authors have developed a new phantom and an associated calibration

method designed for quantitative evaluation of MEG systems⁷⁾. This phantom was calibrated and its uncertainty was determined so as to ensure reproducibility and reliability.

In this paper, an evaluation method for a room-temperature magnetic sensor using the calibrated phantom is introduced. As an example of the experimental evaluation with the phantom, we chose a magneto-impedance (MI) sensor that is a candidate for realizing a helium-less MEG system. The experimental setup is detailed in Section 2. The measured data are presented in Section 3. The feasibility of MEG signal detection by the MI sensor is discussed in Section 4.

2. Method

2.1 Phantom

One popular method to analyze the MEG data is to estimate a magnetic source in a human brain using the Sarvas formula⁸⁾. In the model of the Sarvas formula, the human brain and the source current are a conductive sphere and a current dipole, respectively. There are two types of phantoms: one is the “wet phantom”, composed of two electrodes installed in a sphere filled with saline, and the other is the “dry phantom”, composed of a triangular wire based on Ilmonieimi’s suggestion⁹⁾. We have chosen the dry-type phantom because it is much easier to handle, maintain, and calibrate.

Figure 1 shows the schematics of the phantom. Two individual isosceles triangles were wound around a quadrangular pyramidal bobbin. The isosceles triangular model has a 5-mm base and 65-mm height. Twenty-five bobbins were assembled inside a domed cover that imitates a human skull. The equivalent current dipoles (ECDs) corresponding to fifty triangular

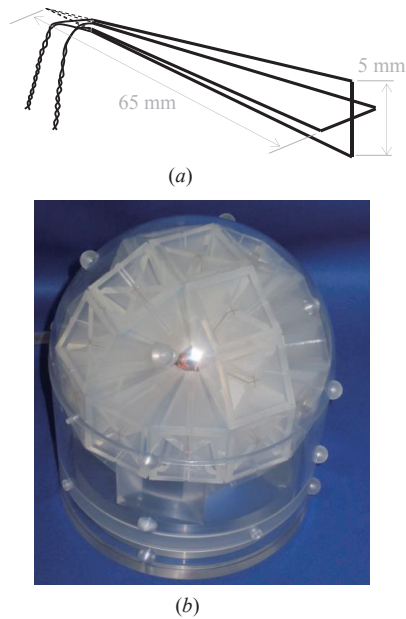


Fig. 1 Configuration of the MEG phantom. (a) schematic of an isosceles-triangular coil pair. (b) photograph of the MEG phantom⁷.

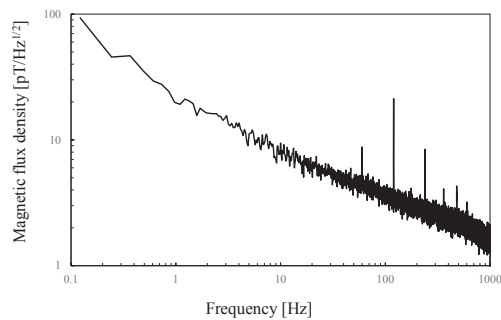


Fig. 2 Noise level of the MI sensor recorded inside a magnetically shielded room.

wires were estimated based on three-dimensional measurement of the current paths and numerical calculations. The details of the phantom configuration and calibration are described in Ref. 7.

2.2 Sensor

In this study, we used a commercially available MI sensor (MI-CB-1DH, Aichi Micro Intelligent Corporation). Figure 2 shows the magnetic noise spectrum recorded inside a magnetically shielded room (MSR). The noise level was approximately 10 pT/Hz^{1/2} at 10 Hz. The noise level of a SQUID sensor for an MEG system should be of femto-Tesla order. Although the sensitivity of the MI sensor is insufficient, the room-temperature sensor has the advantage of being placed at a closer position to the head. Improvement of the signal-to-noise ratio is expected because of the shorter distance between the sensor and the signal source.

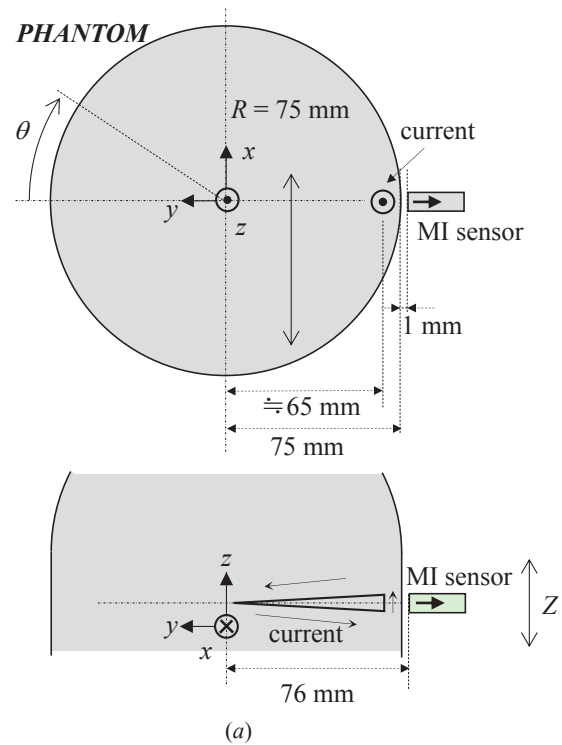


Fig. 3 Setup for experimental evaluation of the MI sensor using the phantom. (a) Schematics of the experimental setup and (b) photograph of the phantom and the MI sensor.

2.3 Experimental setup

Figure 3 shows (a) the experimental setup and (b) the photograph of the phantom and the MI sensor. One triangular wire was chosen for the experiment and an electric current was applied to it by a function generator. The waveform was a sinusoidal burst at a frequency of 11 Hz. The measurement was performed using different current amplitudes $I = 10$ and $100 \mu\text{A}$. The intensity of the ECD corresponding to an applied current amplitude of $10 \mu\text{A}$ was approximately 50 nA m. This ECD intensity is similar to that estimated from the recorded data of human auditory evoked responses.

To measure the magnetic field distribution near the phantom, the MI sensor and the phantom were fixed on a three-axial stage and a rotation stage, respectively. The sensing direction of the MI sensor was indicated by arrows in Fig. 3, therefore, the magnetic field normal to the phantom surface was detected by the MI sensor. The total number of measuring points was 54; these

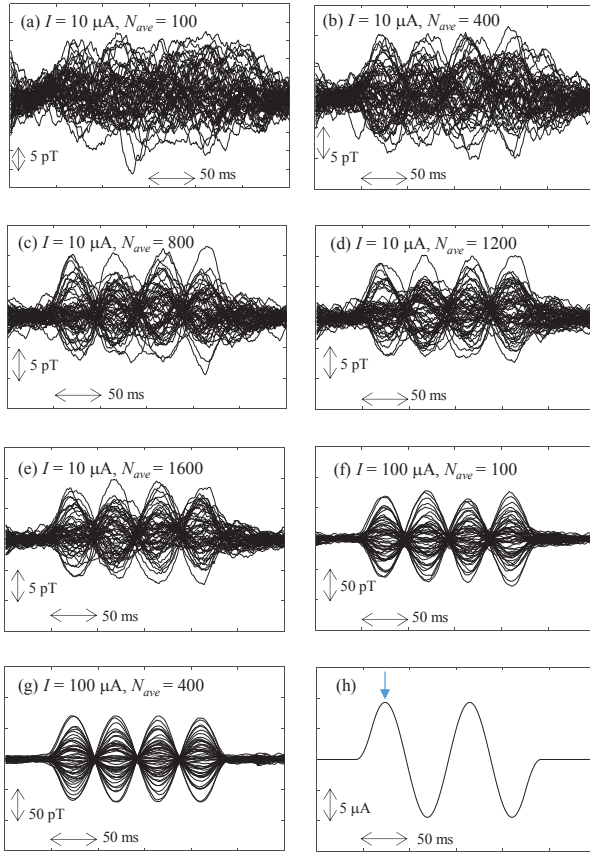


Fig. 4 Measured waveforms (a)-(g) with different current amplitudes (I) and averaging numbers (N_{ave}), and the applied current waveform (h).

points were obtained by rotating the phantom ($\theta = 0^\circ, \pm 4^\circ, \pm 12^\circ, \pm 20^\circ, \pm 28^\circ$) and vertically shifting the MI sensor ($z = -20, -10, 0, 10, 20, 30 \text{ mm}$). The phantom and the MI sensor were placed in an MSR while measurements were taken.

The output signal of the MI sensor was amplified ($\times 1000$) and band-pass filtered (cut-off frequencies = 0.1 Hz and 500 Hz) before recording. The recording was performed by a 16-bit A/D converter (PCIe-6353, National Instruments). The sampling frequency was 2000 Hz , and the recording time was 440 s for $I = 10 \mu\text{A}$ and 120 s for $I = 100 \mu\text{A}$. After recording, the waveforms were averaged to reduce noise just as in the case we measure a human evoked response. We applied different averaging numbers, namely, 100, 400, 800, 1200, and 1600 for $I = 10 \mu\text{A}$, and 100 and 400 for $I = 100 \mu\text{A}$, so as to consider different signal-to-noise ratios. Moving-average processing was also conducted with a window length of 16.5 ms to reduce power-line interference (60 Hz). Then, source localization using the Sarvas formula was conducted for each data set.

3. Result

Figure 4 shows the waveforms of measured data and applied current in (h). The measured waveforms in

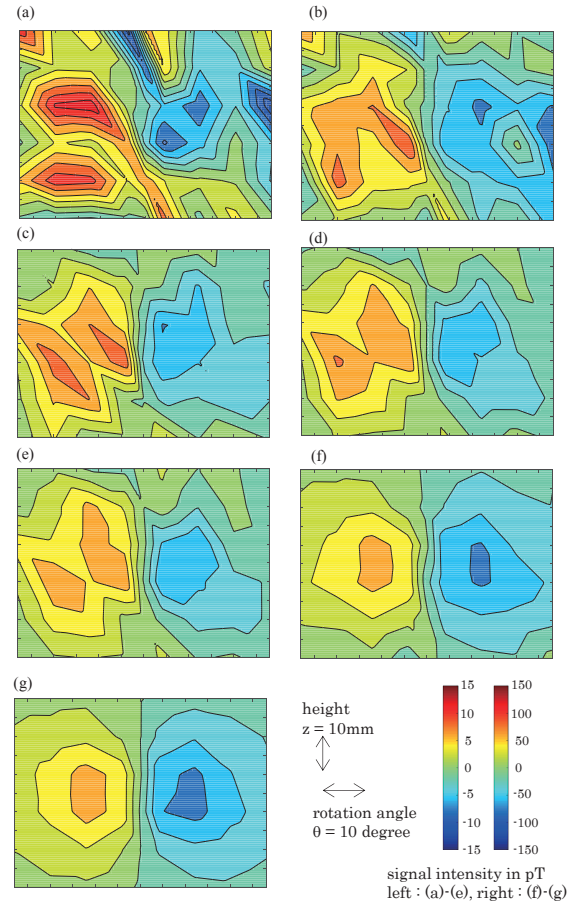


Fig. 5 Contour maps with different current amplitudes (I) and averaging numbers (N_{ave}).

(a)-(g) correspond to different averaging numbers and applied current amplitude 100, 400, 800, and 1600 for $I = 10 \mu\text{A}$, and 100 and 400 for $I = 100 \mu\text{A}$, respectively. The waveform detected at 54 measuring points is overlapped. The applied current waveform when $I = 10 \mu\text{A}$ is shown in Fig. 4 (h).

Figure 5 shows the contour maps of the measured magnetic field distributions. Figure 5 (a) - (g) are the same as those of Fig. 4. The time point of the displayed data was the first peak of the sinusoidal waveform, indicated by a triangular arrow in Fig. 4(h).

The source estimation was conducted using a least-mean-square method and the Sarvas formula. Figure 6 shows the source localization error and goodness-of-fit (GOF) value in the estimation. Figure 6(a)-(g) are the same as those of Figs. 4 and 5. Source estimation was performed at every four peaks of the sinusoidal waveform; the length of the bar indicates the mean value of the source localization error and the GOF. By increasing the signal-to-noise ratio, the source localization error decreased and the GOF increased.

4. Discussion

The amplitude of the magnetic signal from the human brain detected by a SQUID-based MEG system

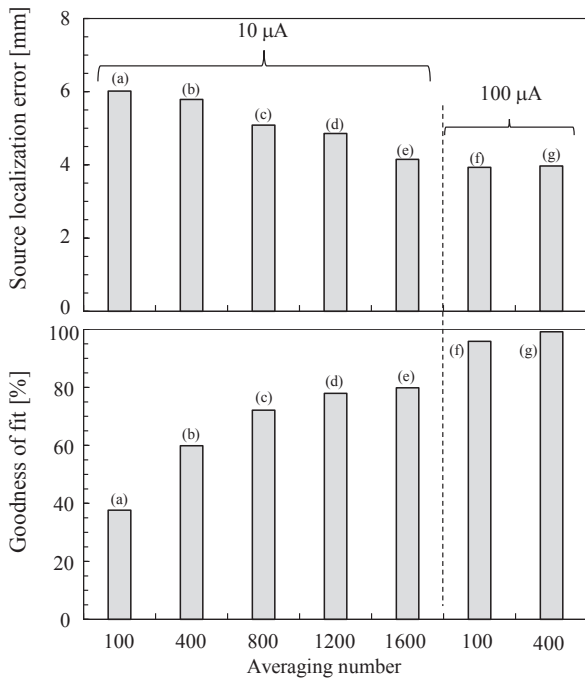


Fig. 6 Source localization error and goodness of fit in ECD analysis.

is typically found to be approximately 1 pT or less. However, larger waveforms, as shown in Fig. 4(e), can be detected by a room-temperature sensor that was located much closer to the target. These results show the possibility of realizing a room-temperature sensor-based MEG system.

When a new magnetic sensor is developed or the sensitivity of a magnetic sensor is improved, the averaging number used to observe the biomagnetic signal is usually considered a criterion for the evaluation of its performance. As shown in Fig. 6, the source localization error with different averaging numbers can be obtained using the phantom. For example, we conclude that 4.2 mm of accuracy and 80% of GOF can be achieved with 1600-times averaging for MEG measurements when using the MI sensor.

In the case of MEG measurement using a SQUID-based system, the averaging number is usually set to approximately 100, in consideration of the trade-off between signal-to-noise ratio and fatigue and/or the duration of concentration of a subject. In contrast, we choose 1600-times averaging as a maximum to obtain a better signal-to-noise ratio. One of the benefits of using the phantom is high reproducibility of the measurement result with a high signal-to-noise ratio based on long-duration measurement.

Furthermore, we also carried out measurements at a current amplitude of 100 μ A such that the signal amplitude was 10-times-larger than the human MEG signal. The obtained signal-to-noise ratio is equivalent to that with a 100-times-larger averaging number

because the noise decreases in proportion to the square root of the averaging number. Therefore, the results in Fig.6 (f) and (g) correspond to the source localization errors and GOF values at an averaging number of 10000 and 40000 for $I = 10 \mu$ A, respectively. By applying a large electric current to the phantom, we can obtain a result equivalent to using a large averaging number. From these results, another conclusion is obtained: 4.0 mm of accuracy and over 99% of GOF can be achieved with 400-times averaging if the sensor noise decreases to 1/10. These conclusions provide the target specifications of the room-temperature magnetic sensors used to realize MEG measurements.

In addition, we should point out the value of the source localization error. In this experiment, the smallest source localization error was 4.0 mm when $I = 100 \mu$ A and the averaging number is 400. This error was much larger than that obtained by the SQUID-based MEG systems⁷⁾. A lower signal-to-noise ratio, smaller measuring points, and a lack of accuracy of sensor positioning are considered to be the causes of the larger source localization error. Specifically, the accuracy of the sensor positioning is supposed to be the major cause of the source localization error because there is a large magnetic field gradient near the signal source comparing with that of SQUID-based MEG systems¹⁰⁾. It is also important to accurately calibrate the sensor position and orientation to realize the MEG system.

5. Conclusion

We demonstrated the experimental evaluation of the MI sensor using the calibrated MEG phantom. The signal source was estimated from the observed magnetic field distribution at different signal-to-noise ratios. The results showed the possibility (and difficulty) of realizing MEG measurements using the MI sensor. The use of the calibrated phantom is effective for evaluating the performance of magnetic sensors.

Acknowledgements This research was partly supported by The Hokuriku Industrial Advancement Center.

References

- 1) S. Yabukami, K. Kato, T. Ozawa, N. Kobayashi, and K. I. Arai: *J. Magn. Soc. Jpn.*, **38**, 25 (2014).
- 2) H. Karo, and I. Sasada: *J. Appl. Phys.*, **117**, 17B322 (2015).
- 3) T. Yamamoto, K. Tashiro, and H. Wakiwaka: *The Papers of Tech. Meeting on "Magnetics"*, MAG-15-9, 41 (2015).
- 4) H. Xia, A. B-A. Baranga, D. Hoffman, and M. V. Romalis: *Appl. Phys. Lett.*, **89**, 211104 (2006).
- 5) K. Wang, S. Tajima, Y. Asano, Y. Okuda, N. Hamada, C. Cai, and T. Uchiyama: *Proc. of the 8th Intl. Conf. on Sens. Tech.*, 547 (2014).
- 6) Y. Ando: *Journal of Japan Biomagnetism and Bioelectromagnetics Society*, **29**, 20 (2016)
- 7) D. Oyama, Y. Adachi, M. Yumoto, I. Hashimoto, and G. Uehara: *J. Neurosci. Methods*, **251**, 24 (2015).
- 8) J. Sarvas: *Physics in Medicine and Biology*, **32**, 11 (1987)
- 9) R. J. Illmonieimi, M. S. Hamalainen, and J. Knuutila: in

Proc. Biomagnetism: Applications & Theory, New York, Pergamon, 278 (1985)

- 10) D. Oyama, Y. Adachi, and G. Uehara: *The Papers of Technical Meeting on "Magnetics"*, IEE Japan, MAG-16-1 (2016)

Received Dec. 22, 2016; Revised Mar. 13, 2016; Accepted Apr. 05, 2017